

Towards Accessible Fabrication of Proprioceptive Soft Robotic Tentacles Without External Sensors

Josephine Koe



Electrical Engineering and Computer Sciences
University of California, Berkeley

Technical Report No. UCB/EECS-2022-81

<http://www2.eecs.berkeley.edu/Pubs/TechRpts/2022/EECS-2022-81.html>

May 12, 2022

Copyright © 2022, by the author(s).
All rights reserved.

Permission to make digital or hard copies of all or part of this work for personal or classroom use is granted without fee provided that copies are not made or distributed for profit or commercial advantage and that copies bear this notice and the full citation on the first page. To copy otherwise, to republish, to post on servers or to redistribute to lists, requires prior specific permission.

Acknowledgement

I would like to acknowledge and express my appreciation to my advisor Professor Shankar Sastry and reader Professor Yi Ma for their guidance and support throughout the course of this work. This project would not have been possible without them and I am very grateful to have had the opportunity to learn from them.

I would also like to thank my friends and family for their endless encouragement and patience throughout this journey. Your support has strengthened me countless times and I would not have earned this degree without you.

**Towards Accessible Fabrication of Proprioceptive Soft Robotic
Tentacles Without External Sensors**

by Josephine Koe

Research Project

Submitted to the Department of Electrical Engineering and Computer Sciences,
University of California at Berkeley, in partial satisfaction of the requirements for the
degree of **Master of Science, Plan II.**

Approval for the Report and Comprehensive Examination:

Committee:



Professor Shankar Sastry
Research Advisor

May 3, 2022
(Date)



Professor Yi Ma
Second Reader

May 9, 2022
(Date)

Towards Accessible Fabrication of Proprioceptive Soft Robotic Tentacles Without External Sensors

Josephine Koe

May 12, 2022

Abstract

Soft and flexible robotic manipulators can easily adapt to a variety of environments due to their compliance. Although this flexibility can be a huge advantage in many situations, soft robots have infinite degrees of freedom and are difficult to control. In addition, few soft manipulators have been created that are capable of proprioception without external sensing, and those that have this capability often require very precisely manufactured sensors. This work presents an analysis of four easily manufactured or purchased sensors, design and fabrication of a soft tentacle actuator, and the integration of embedded sensors into the soft robotic system with the goal of proprioceptive capabilities.

1 Introduction

Soft robots are made out of materials that are intrinsically soft, extensible, or both. Their compliance makes them ideal for situations involving unknown environments and objects. In particular, soft robots are very fitting for applications that require close contact with humans because they can deform and absorb much of the energy that comes with a collision [1]. Soft tentacles are able to flexibly maneuver around narrow passageways and obstacles, making them useful tools in applications such as minimally invasive surgery [2].

While the compliance of soft robots makes them versatile manipulators, this attribute also makes such robots difficult to control. Because soft robots deform along their entire length, they essentially have infinite degrees of freedom. Many control schemes for rigid-body robots utilize feedback, which requires knowing or observing values that represent the robot's state. Likewise, this ability of sensing one's state, also known as proprioception, is valuable in the task of controlling soft robots.

Like traditional rigid-body robots, soft robots are made up of actuators and sensors. These components must provide motion and perception capabilities respectively while maintaining the soft properties of the robot. There are a variety of options for these components, each with their own advantages and challenges.

1.1 Actuation

An actuator produces a physical motion that can be rotational, translational, or both. The compliance of soft robots requires soft actuators to behave very differently from traditional rigid actuators. Some common types of soft actuators are tendon-driven actuators, hydraulic actuators, and pneumatic actuators.

Tendon-driven continuum robots are driven by applying tension on cables that pass through an elastic structure, making it contract along the length of the cable [3]. For example, Calisti et al. designed a robotic system that can use a steel cable to vary the length of the arm and a Dyneema[®] fibre cable to bend the arm to mimic certain muscles of an octopus [4]. Tendon-driven continuum robots with a thin form factor are well-suited for applications such as minimally invasive surgery where long, flexible surgical instruments can be inserted into the body through small incisions or natural orifices for increased patient safety [5].

Hydraulic actuators fill flexible chambers within the soft robot with liquids to expand the chambers in certain directions. Once the fluid is inside the robot, the pressure does not need to be continuously applied due to the incompressibility of liquids. Because of this, hydraulic actuators are capable of exerting much more force than similarly-sized pneumatic actuators. However, hydraulic actuators tend to be more expensive than pneumatic actuators [6].

Pneumatic actuators are similar to hydraulic actuators in that they move the robot by filling spaces with certain amounts of fluid; the difference is pneumatic actuators use gas instead of liquid. One example of a pneumatic actuator is a pneumatic network (PneuNet), which is a combination of channels and chambers within an elastomer. When inflated, expansion occurs in the most compliant regions. Designers can easily pre-determine the actuator's behavior by selecting different wall thicknesses or materials for specific regions [7]. These actuators are also fairly easy to manufacture. Another common pneumatic actuator is the McKibben artificial muscle [8], which inflates an inner bladder within a sheath that contracts lengthwise when expanded radially [9]. These actuators are very efficient in that they provide a large amount of force for their weight [10].

1.2 Sensing

Sensors for soft robots can be classified as proprioceptive, exteroceptive, or both. Proprioceptive sensors, such as stretch sensors attached to the inflatable part of a soft robot, measure the state of the robot itself. On the other hand, exteroceptive sensors, such as a pressure sensor placed at the robot's end-effector where it will come into contact with obstacles, gather information about the environment the robot is in. Since proprioception is useful in the task of controlling the robot, this work focuses on proprioceptive sensors which can be further split into embedded sensors and external sensors. Embedded sensors, such as pressure sensors in the inflatable chambers in a soft robot, are placed within the robot. External sensors, such as a camera that is outside of the robot but pointing at the robot to view what it looks like, are placed in the environment that the robot is in. The use of external sensors limits the usability of a robot by limiting the possible environments the robot can be used in to those that have the sensors in them, so this section will only focus on proprioceptive embedded sensors. Examples of these include wire braids, inertial

measurement units, and piezoresistive sensors.

Wires braids can be wrapped around a soft robot and conform to its shape such that when it moves, the inductance between the wires changes. Based on the difference in inductance from the resting position, it is possible to determine the current position of the robot with accuracy comparable to IMU data [11]. The simplistic design of this sensor only requires simple, inexpensive wires and allows for easy installation and adds minimal infrastructure to the robot. However, the best results occur with smaller diameters of the coils which limits the ease of manufacturing of the actuator part of the tentacle [11]. Inductance sensors also can be susceptible to electromagnetic interference.

Inertial measurement units (IMUs) use accelerometers and gyroscopes to determine the position and orientation of the unit. IMUs are small enough to be placed on or within soft, deformable objects to be used for pose estimation [12]. However, these units are not intrinsically soft or stretchable and their readings can be susceptible to drift where errors at each time step build up on each other [11].

Piezoresistive materials change in resistance when an external stress is applied to it [13]. Deformations in a piezoresistive material can be sensed by measuring the resistance across it [14]. This property can be utilized by laser-cutting sheets of piezoresistive material so they are stretchable and can be bonded to a soft robot [15]. These piezoresistive materials are ideal for soft applications because they are flexible and stretchable, but they are susceptible to hysteresis and can be less accurate than some of the other sensors used in these applications.

One drawback among many different types of soft sensors is that accuracy can come at the cost of precise manufacturing with expensive and not-easily-accessible equipment. This work aims to address this issue by designing a soft tentacle that is easily manufactured from off-the-shelf materials and is capable of proprioception.

2 Embedded Sensors

The first part of this work provides an analysis of different types of easily bought or manufactured sensors for soft robots.

2.1 Carbon Fiber Sensors

One of the types of self-manufacturable sensors tested in the course of this work was made of carbon fiber. These sensors were made by first dissolving chopped carbon fiber in rubbing alcohol to separate the fibers into individual strands. These strands were then mixed into silicone before it cured. After the silicone was cured, the resulting material was both conductive and flexible, and this process can easily mold sensors as any shape (Figure 1a). Measuring the resistance across this material can provide an indication of how much the material has deformed.

Even with these properties, this type of sensor had a number of issues. Embedding carbon fiber strands into the silicone significantly reduced the intrinsic stretchability of the silicone. This made them extremely impractical for the intended usage of being manufactured as strips to be attached to the side of an extendable tentacle. As stretch sensors, they were

also quite prone to hysteresis which would make it even more difficult for them to accurately measure the extent that they had been stretched.

Although these sensors did not perform well as stretch sensors, they did show some promise as tactile pressure sensors. This is due to the electrical properties of polymer/carbon nanotubes nanocomposites which display a negative piezoresistance effect under pressure where the resistance of the material decreases with an increase in pressure [16]. However, since tactile pressure sensors are exteroceptive sensors, the performance of these sensors as tactile pressure sensors was not seriously explored in this work.

2.2 Iron Powder Sensors

The other type of sensor that was manufactured as a part of this work utilized the conductive properties of iron powder. Combining iron powder and conductive EMG gel creates a conductive mixture that can be spread on the side of a soft robot and changes in resistance when deformed like the carbon fiber sensors (Figure 1b).

Before the EMG gel dried, the mixture did have variable resistance. However, the EMG gel would dry out within a few days and the iron powder would become brittle and start peeling off the side of the robot, making this sensor extremely impractical for long-term use. There were also a few attempts made at mixing iron powder into silicone before it cured, but this did not make the silicone conductive and instead made the material more rigid. Given these major drawbacks, this type of sensor was not explored much further past the manufacturing stage.



(a) Carbon fiber sensors

(b) Iron powder sensors

Figure 1: Self-manufactured sensors of different sizes and shapes.

2.3 Conductive Rubber Cords

One of the off-the-shelf sensors explored in this work was the Adafruit Conductive Rubber Cord Stretch Sensor (Figure 3a). These sensors are 2 mm diameter cords made of carbon-black impregnated rubber, so they are both stretchy and conductive. This material has piezoresistive properties in that its resistance changes as the cord is stretched [17].

According to the manufacturer’s website, the resistance of the cord should be about 350 ohms per inch. As the cord is stretched, the resistance of the cord should increase with an approximate but not a true linear relationship. The rubber can be stretched about 50-70% longer than its resting length, making this material a good fit for being attached to a soft and stretchy material to measure its length. However, because the resistance of the material may vary between manufacturing batches, it is reported to not be precise [17].

These reported specifications did not exactly match the results of experiments with this sensor in this work. Most significantly, it was found that the resistance of the cord decreases as the cord is stretched. The experimental data displayed in Figure 2 roughly indicates an exponential relationship, but more work must be done to accurately characterize the relationship between stretch length and resistance of these cords.

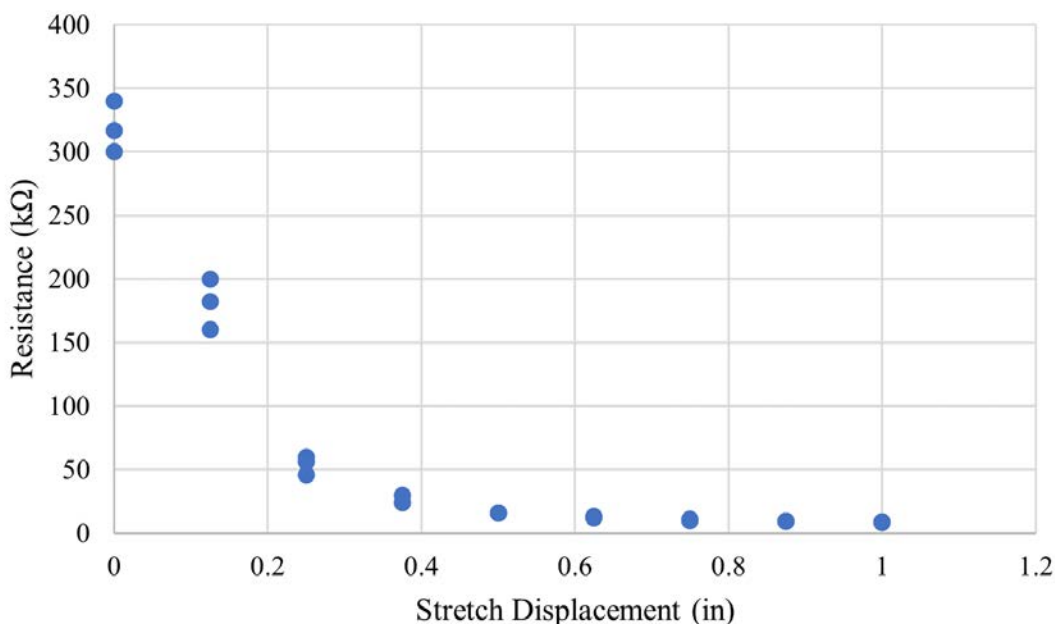


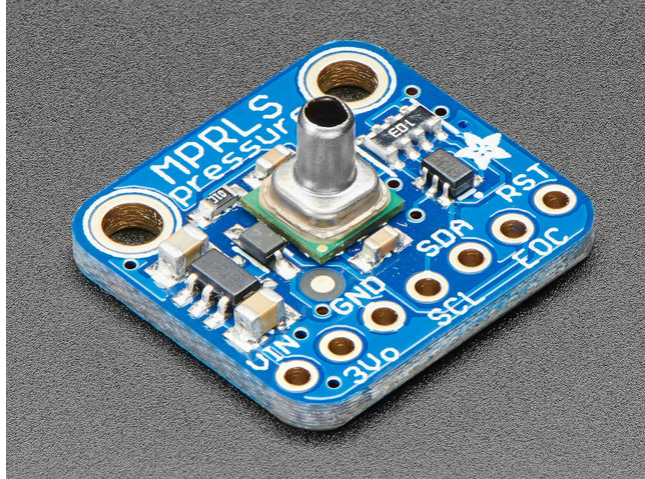
Figure 2: Measured resistance at various stretch displacements across a cord with a resting length of 2 in.

2.4 Air Pressure Sensors

While an air pressure sensor is not made of soft materials, it can be connected to the air tubing that leads out of the soft robot. In general, air pressure sensors can be used as an indicator of how much an inflatable cavity has been inflated which, if given an accurate model of the inflation behavior of the cavity, can be converted into a measurement of its pose. This work utilized the Adafruit MPRLS Ported Pressure Sensor Breakout (Figure 3b) which can measure air pressures of 0-25 psi [18].



(a) Conductive rubber cord [17]



(b) Pressure sensor [18]

Figure 3: Off-the-shelf sensors.

3 Design

The design of the tentacle was based on the following requirements:

- **The tentacle should have more than one independent soft segment.** In order to create shapes with varying curvature, the tentacle should be broken up into multiple segments that can be actuated independently.
- **Each segment of the tentacle should be capable of rotation in 3D space.** Each segment should be able to actuate in any direction that it can physically bend in to span the entire reachable workspace of the robot.
- **Each segment should be easily attachable to the previous one.** For ease of use, extending the tentacle should not require extensive changes in the design of its segments.
- **The tentacle should only utilize embedded sensors.** Once calibrated, the tentacle should not require external sensors to be situated in the environment in order to operate.
- **The tentacle should be reasonably easy to fabricate.** Making the tentacle should not require expensive or particularly high-precision equipment. Ideally the tentacle will use off-the-shelf parts that are easy for anyone to obtain.

Extensive iteration was done on the design of the tentacle based on these requirements.

3.1 Actuation

This work explored different designs for pneumatic actuators. Pneumatic actuators were chosen over hydraulic actuators for their lower price and less detrimental consequences for

the robot in the event of a leak. While hydraulic actuators provide more rigidity than pneumatic actuators, air can travel faster than liquid due to the inherent inertia and drag of liquids so pneumatic actuators would provide faster responses than hydraulic actuators.

This section describes the main stages of the actuator design iterations throughout this work. Since one of the design requirements was that each segment should be capable of rotation in 3D space, early iterations of the tentacle segment comprised of three PneuNet chambers connected in parallel with each other (Figure 4a). Inflating one or more of the PneuNet chambers resulted in a rotation and some translation of the end-effector from its original orientation (Figure 4b).

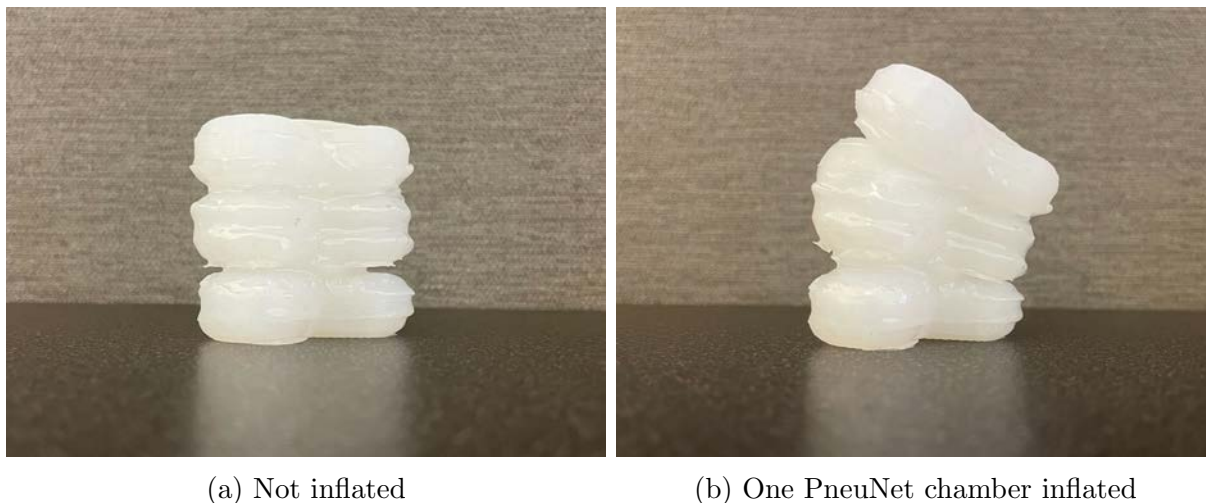


Figure 4: Early tentacle segment prototype.

To increase the range of rotation, the axial length of the tentacle segment was increased to be at least thrice the diameter of the segment's cross-section. While this would make the behavior of the tentacle more susceptible to external forces given the longer moment arm, it made the movements more exaggerated for testing purposes (Figure 5). When the segment was suspended vertically, the longer length allowed it to hold but not crush a delicate paper box as a demonstration of the advantages of soft actuators (Figure 5d).

When a satisfactory tentacle segment design was reached, two of such segments were connected together to form the first prototype of a multi-segment tentacle. The segments were connected such that the movement generated from inflating one chamber in the first segment from the point of suspension could be opposed by inflating another chamber in the second segment from the point of suspension, creating the spline shape in Figure 6a.

The first multi-segment prototype illuminated a number of issues to be addressed. The main one was that the tubing that provided air to the second segment from the point of suspension was outside of the tentacle and could potentially get caught on objects in the environment. This prompted the next iteration of the design to include a channel through the center of the tentacle segment that the tubing can pass through and be contained within. The second major improvement that was made was that the shape of the variable thickness walls was inverted so the outer side of the wall was smooth and the inner side of the wall had the periodic reinforced sections. This made the tentacle segment more stable by removing

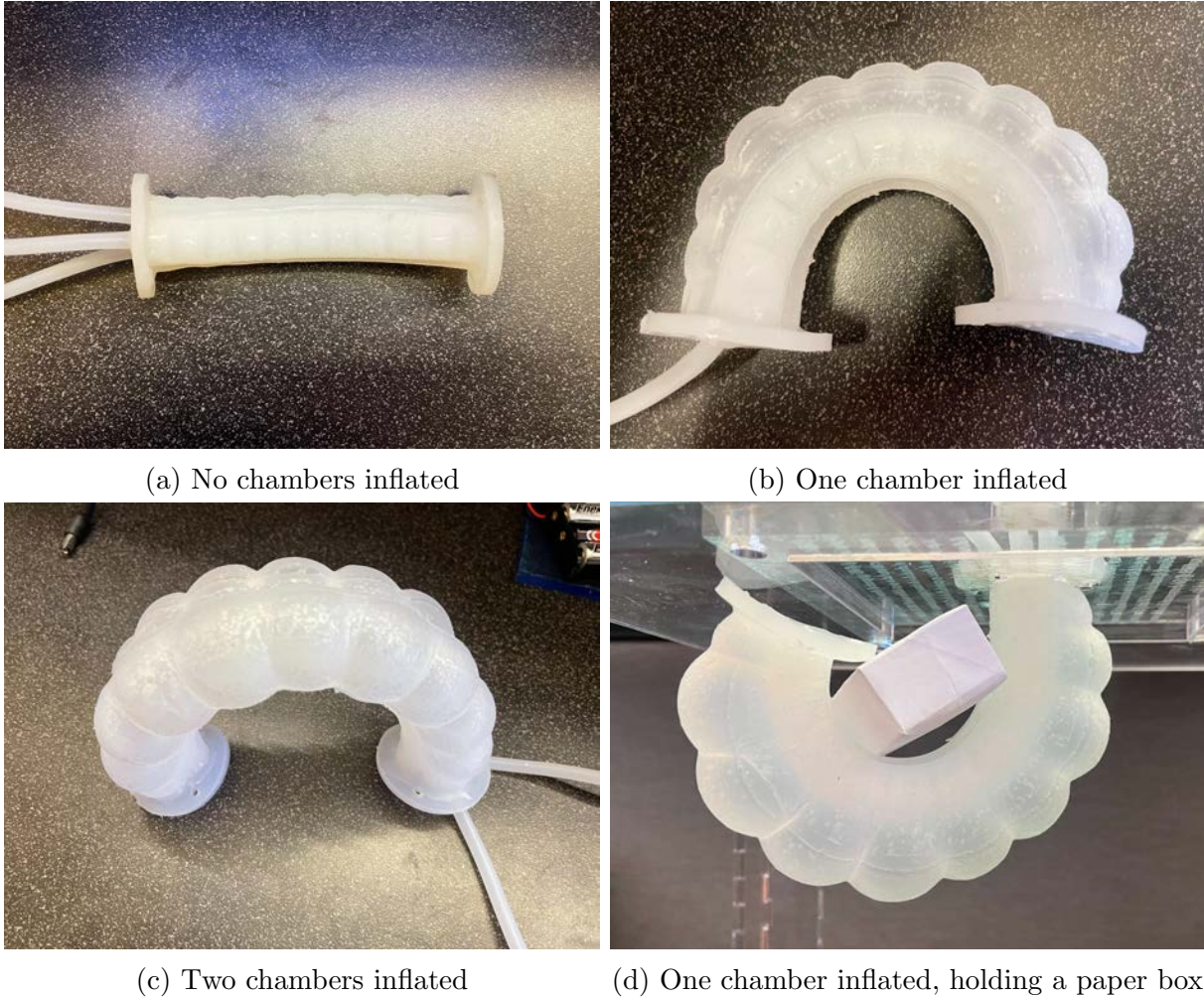
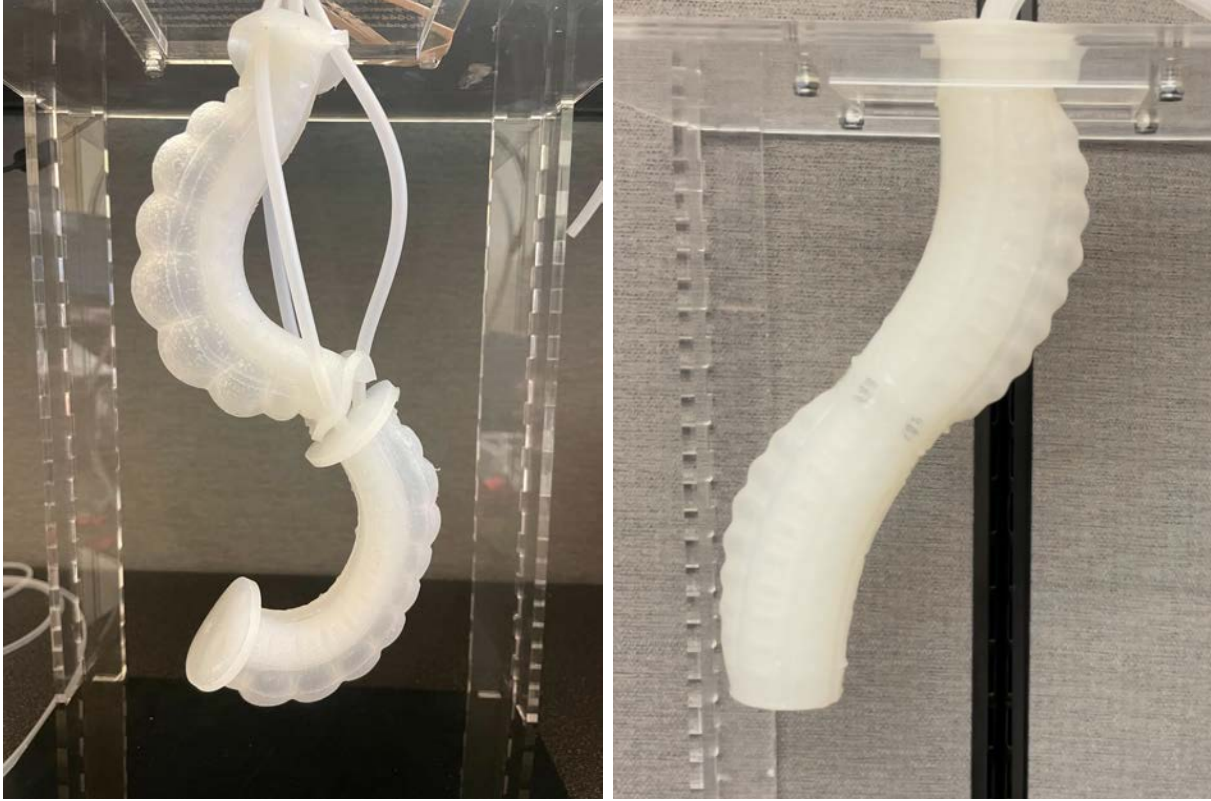


Figure 5: Longer tentacle segment prototype.

the natural bending points along the side of the segment in addition to making the form factor of the segment more smooth. Another change that was made in the final design was the creation of six chambers per segment instead of three even though there were still only three being inflated. This design choice made the chambers thinner, prompting the inflation to be more prominent in the axial direction than in the radial direction as desired. Creating six chambers per segment also made it easier to align opposing chambers in consecutive segments. The final multi-segment tentacle design can be seen in Figure 6b.

The inflation of the tentacle can be controlled by a user. The user interface circuit has six sliding potentiometers that correspond to the six inflatable chambers. When the user moves the slider to the extreme ends of the potentiometer, the Arduino Uno commands the corresponding pump and release valve to inflate or deflate the chamber accordingly (Figure 7). Otherwise, neither the pump nor the valve are powered and the chamber for the most part holds the air in it and holds its position. The pumps are powered at only a 50% duty cycle because they are not rated for continuous use [19].



(a) First multi-segment tentacle prototype (b) Final multi-segment tentacle prototype

Figure 6: Multi-segment tentacle prototypes.

3.2 Sensing

Based on the analysis in the previous section, the conductive rubber cords and air pressure sensors were chosen to be used in this system. Each inflatable chamber was allocated one air pressure sensor to measure the extent of inflation of that chamber. In addition, three conductive cords were wrapped along the sides of the tentacle between the inflatable chambers. A single grounded contact point connected the cords at the end of the tentacle, creating six lengths of conductive cord around the tentacle that were each connected to a voltage divider. An additional contact point was also inserted at the midpoint of each of the six lengths. These points were programmed to alternate between floating and ground values, allowing measurements of voltage across both the entire cord length and one half of the cord length in the voltage divider. For each cord, the value read from the voltage divider can be converted to a resistance value which provides an indication of the length of that cord. Altogether, this setup provided six length measurements for each of the two tentacle segments. Although theoretically only three lengths would be required to reconstruct a constant curvature segment in 3D space, using six lengths provides redundancy for better accuracy.

The sensing circuit can be seen in Figure 8. The Arduino Unos use the I2C protocol to read data from the six pressure sensors which each read the pressure inside the air tubing for one of the chambers. The off-the-shelf breakout board for the pressure sensor has a pre-programmed I2C address, so an I2C multiplexer board must be used to retrieve the values

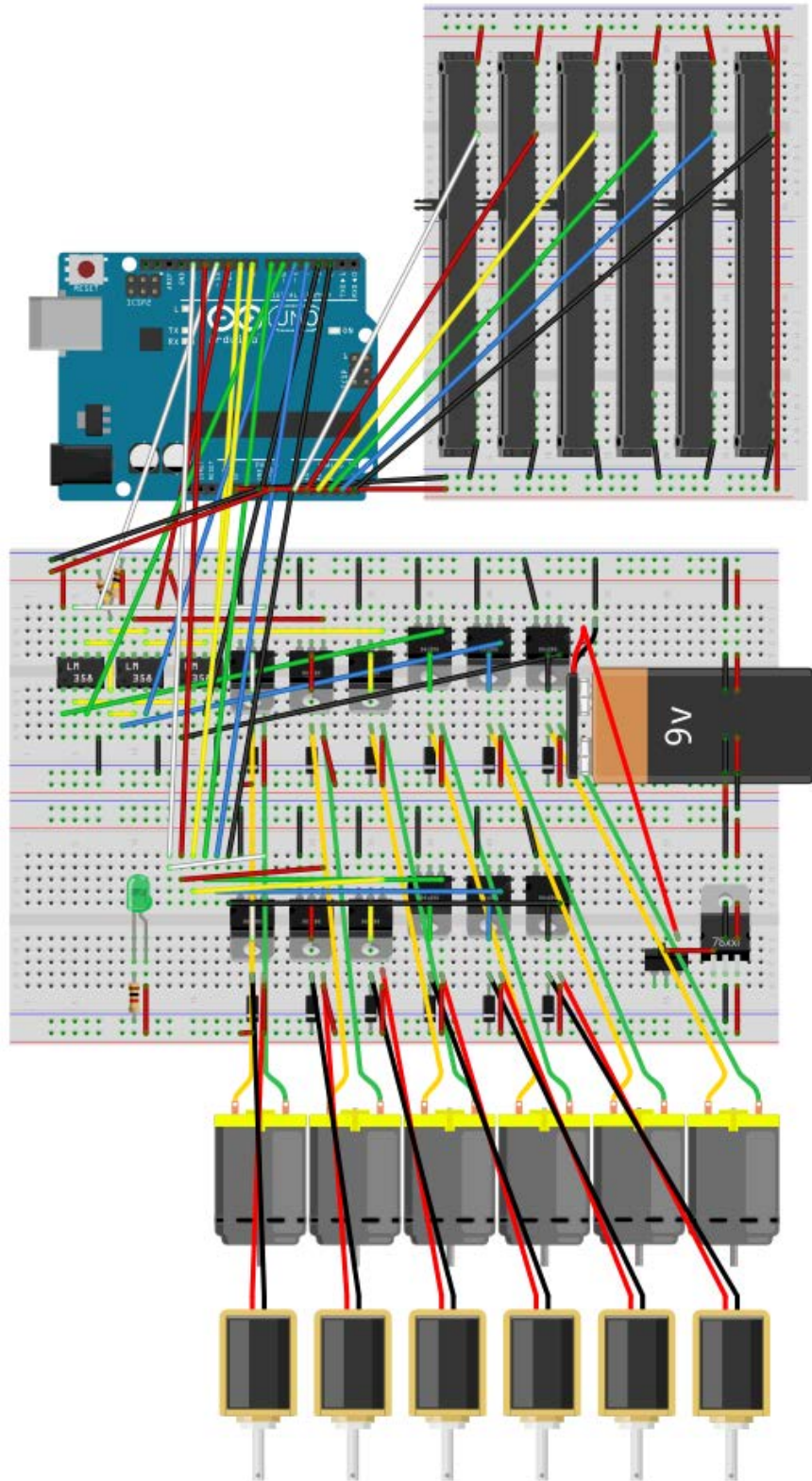


Figure 7: Breadboard diagram of the user interface circuit.

from all of the pressure sensors. A second Arduino Uno was also necessary because even though there are six analog pins on the Arduino Uno, two of them correspond to the data and clock lines for I2C communication so those two functions cannot be used at the same time.

Table 1 presents the bill of materials for the notable components of the design, excluding parts that are commonly found in an electronics lab. The total cost of this tentacle is comfortably under \$500, making this an affordable soft robotic experimental platform.

Table 1: Bill of materials for notable design components.

Part	Quantity	Price	Total
Dragon Skin 10	1	41.16	41.16
Air Pump	6	7.95	47.70
Air Valve	6	2.95	17.70
4mm OD Tubing	1	12.49	12.49
Tee Connector (Pack of 5)	2	6.99	13.98
Arduino	3	18.99	56.97
Conductive Rubber Cord	3	9.95	29.85
Pressure Sensor	6	14.95	89.70
I2C Multiplexer Breakout	1	6.95	6.95
Total			316.50

4 Fabrication

To manufacture the soft actuator design, negative molds of the tentacle segment parts were designed, 3D printed, and assembled (Figure 9). Then Dragon Skin 10 silicone was mixed and poured into the molds. After curing, the silicone parts were removed from the molds. More silicone was mixed and spread on the separate silicone parts to bond them together. After the tentacle segment was fully assembled, the tubing and wires were inserted into the segment and bonded with more silicone. Then the tentacle segments were attached in series by bonding them together with more silicone.

Dragon Skin 10 silicone was chosen as the material for the tentacle based on a very preliminary analysis and trial and error. Out of all of the traditional silicone materials tested in this work (Ecoflex 10, Ecoflex 30, Ecoflex 50, Dragon Skin 10, and Dragon Skin 30), Dragon Skin 10 was chosen because of two metrics: elongation at break and tensile strength. Dragon Skin 10 has a tensile strength of 475 psi and an elongation at break of 1000% which is the best combination of those metrics for the tested materials (Table 2). This essentially means that Dragon Skin 10 can be inflated the most and is one of the hardest silicone types to break, which made it the most attractive choice for the soft tentacle [20].

To easily attach the conductive cord sensors to the side of the robot, the negative molds were designed to create slots in the side of the tentacle segment that fit the cords. After the segment had been assembled, the cords were laid into the slots and bonded to the tentacle

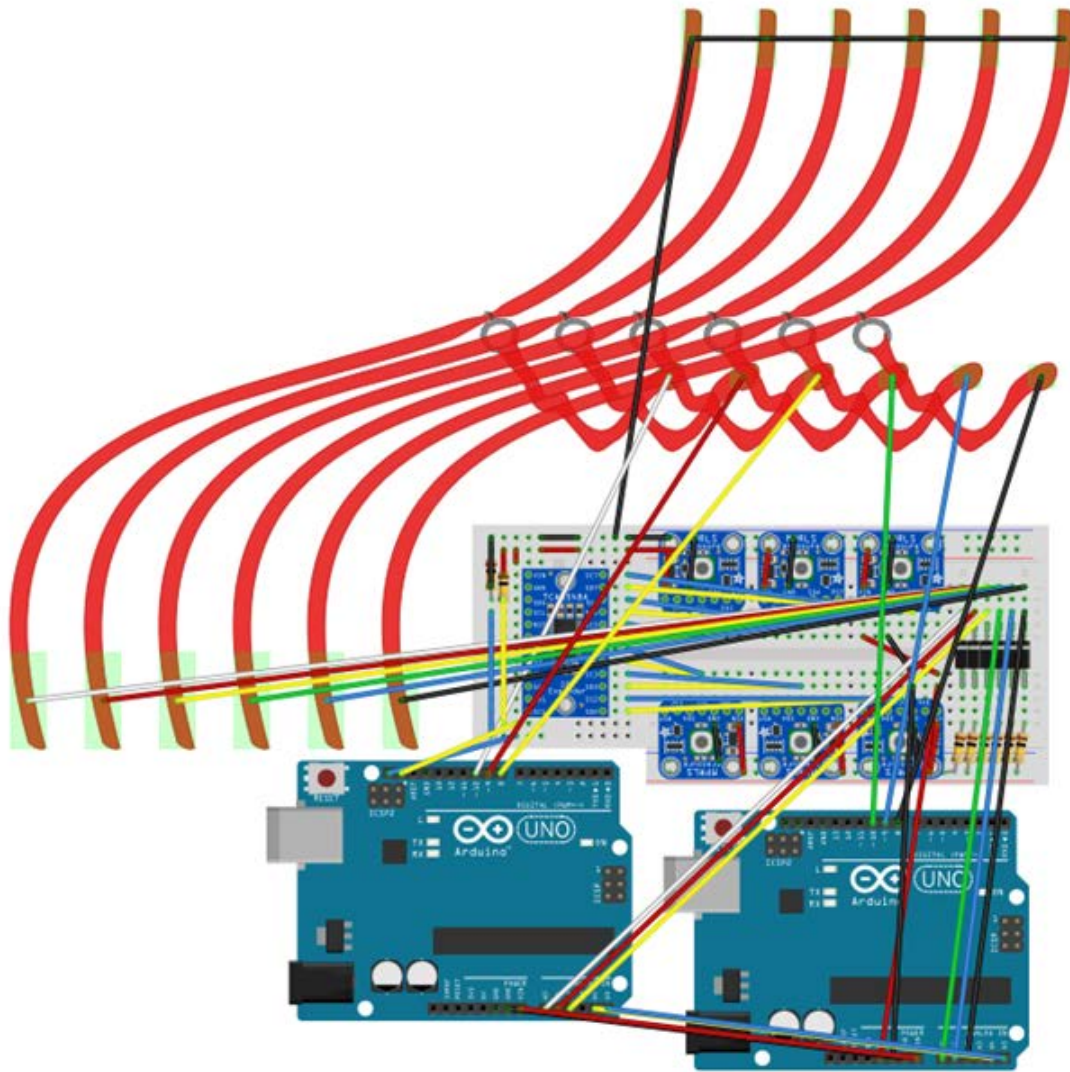


Figure 8: Breadboard diagram of the sensing circuit. The curved red lines in the top left of the image represent the stretch sensors attached to the robot. The Arduino Uno on the right can be connected to a computer to collect sensor data.

Table 2: Comparison of elongation at break and tensile strength of tested silicone types [20].

Silicone Type	Elongation at Break (%)	Tensile Strength (psi)
Ecoflex 10	800	120
Ecoflex 30	900	200
Ecoflex 50	980	315
Dragon Skin 10	1000	475
Dragon Skin 30	364	500



(a) Fully assembled mold (b) Mold with outer shell removed

Figure 9: Negative molds for main tentacle segment part.

with a layer of silicone. This prevented the cords from moving around on the surface of the tentacle or sliding along the slots. The complete soft robotic tentacle can be seen in Figure 10.

5 Modeling

The simplest way to model each segment is to assume that they have constant curvature [21]. Since the tentacle segment can elongate and rotate in 3D space, a segment with constant curvature could be characterized by three quantities:

- L : the axial length of the center of the segment
- q_x : the degree of curvature in one radial direction
- q_y : the degree of curvature in the radial direction orthogonal to q_x

If the sensors provide an accurate measurement of length of the 6 conductive cord segments around each tentacle segment, these three quantities can be computed from those measurements using the formula for arc length

$$s = r\theta \quad (1)$$

where s is the arc length, r is the arc radius, and θ is the degree of curvature of the arc. Assuming constant curvature, Equation 1 can be applied to differences in arc length and arc radius as follows:

$$\Delta s = (\Delta r)\theta \quad (2)$$

The length of the segment L can be calculated by taking the average of the 6 cord lengths. Assuming constant curvature, Equation 2 can be used to show that the cords on opposing sides of the segment should have the same amount of displacement in length so the length of the center of the segment should be the average of the opposing segments. There are three sets of opposing cords and each set should theoretically result in the same center length, so taking the average of all 6 lengths should also give the result of the center length.

Equation 2 can also be used to calculate q_x and q_y . Using the difference in length between one pair of opposing cords and the known distance between the cords, the degree of curvature along the axis between the opposing cords can be calculated as q_x . Likewise, the degrees of curvature along the axes between the other two pairs of opposing cords can be calculated and averaged to get the value of q_y .

Using the values of these three quantities, one can calculate the pose of the end of the tentacle segment in \mathbb{R}^3 . Each of these transformations can be combined to get the overall pose of the tentacle which would make the robot proprioceptive, but it is important to note that this would only be possible if accurate measurements of length could be retrieved from the sensors and this was not sufficiently achieved in this work.

6 Conclusion

This work utilizes an analysis of four different types of sensors in the design of a soft robotic tentacle that only uses off-the-shelf embedded sensors for the goal of proprioception. Carbon fiber nanocomposites were shown to be ineffective as stretch sensors but showed some promise as tactile pressure sensors. Iron powder sensors appeared to be impractical for use with soft robotic tentacles. Instead, off-the-shelf conductive cords and air pressure sensors were incorporated into the design of a soft robotic tentacle. The design met the listed requirements of having multiple segments that can rotate in 3D space and easily attach to each other. In addition, the tentacle design only utilizes embedded sensors and is reasonably easy to fabricate. The chosen sensors provide an indication of what the tentacle's pose is, and if provided with accurate sensor readings this robot could be capable of proprioception without the need for external sensors.

Future iterations of this work could address the difficulty in modeling the relationship of the stretch displacement and resistance of the conductive cords. With an accurate model of the pose of the robot given the sensor readings, this soft robot could be used for closed-loop-control experiments. This soft robotic tentacle is inexpensive and relatively easy to reproduce, so it can be readily manufactured by other researchers to promote more research within the soft robotics field.



Figure 10: Complete soft robotic tentacle.

7 Acknowledgments

I would like to acknowledge and express my appreciation to my advisor Professor Shankar Sastry and reader Professor Yi Ma for their guidance and support throughout the course of this work. This project would not have been possible without them and I am very grateful to have had the opportunity to learn from them.

I would also like to thank my friends and family for their endless encouragement and patience throughout this journey. Your support has strengthened me countless times and I would not have earned this degree without you.

References

- [1] D. Rus and M. T. Tolley, “Design, fabrication and control of soft robots,” *Nature*, vol. 521, no. 7553, pp. 467–475, 2015.
- [2] M. Runciman, A. Darzi, and G. P. Mylonas, “Soft robotics in minimally invasive surgery,” *Soft robotics*, vol. 6, no. 4, pp. 423–443, 2019.
- [3] D. C. Rucker and R. J. Webster III, “Statics and dynamics of continuum robots with general tendon routing and external loading,” *IEEE Transactions on Robotics*, vol. 27, no. 6, pp. 1033–1044, 2011.
- [4] M. Calisti, M. Giorelli, G. Levy, B. Mazzolai, B. Hochner, C. Laschi, and P. Dario, “An octopus-bioinspired solution to movement and manipulation for soft robots,” *Bioinspiration & biomimetics*, vol. 6, no. 3, p. 036002, 2011.
- [5] C. F. Graetzel, A. Sheehy, and D. P. Noonan, “Robotic bronchoscopy drive mode of the auris monarch platform,” in *2019 International Conference on Robotics and Automation (ICRA)*. IEEE, 2019, pp. 3895–3901.
- [6] C. Gonzalez, “What’s the difference between pneumatic, hydraulic, and electrical actuators?” *Machine design*, vol. 17, 2015.
- [7] F. Ilievski, A. D. Mazzeo, R. F. Shepherd, X. Chen, and G. M. Whitesides, “Soft robotics for chemists,” *Angewandte Chemie*, vol. 123, no. 8, pp. 1930–1935, 2011.
- [8] R. H. Gaylord, “Fluid actuated motor system and stroking device,” Jul. 22 1958, uS Patent 2,844,126.
- [9] G. K. Klute, J. M. Czerniecki, and B. Hannaford, “Mckibben artificial muscles: pneumatic actuators with biomechanical intelligence,” in *1999 IEEE/ASME International Conference on Advanced Intelligent Mechatronics (Cat. No. 99TH8399)*. IEEE, 1999, pp. 221–226.
- [10] M. De Volder, A. Moers, and D. Reynaerts, “Fabrication and control of miniature mckibben actuators,” *Sensors and Actuators A: Physical*, vol. 166, no. 1, pp. 111–116, 2011.

- [11] W. Felt, M. J. Telleria, T. F. Allen, G. Hein, J. B. Pompa, K. Albert, and C. D. Remy, “An inductance-based sensing system for bellows-driven continuum joints in soft robots,” *Autonomous robots*, vol. 43, no. 2, pp. 435–448, 2019.
- [12] N. Lin, P. Wu, M. Wang, J. Wei, F. Yang, S. Xu, Z. Ye, and X. Chen, “Imu-based active safe control of a variable stiffness soft actuator,” *IEEE Robotics and Automation Letters*, vol. 4, no. 2, pp. 1247–1254, 2019.
- [13] S. Kon, K. Oldham, and R. Horowitz, “Piezoresistive and piezoelectric mems strain sensors for vibration detection,” in *Sensors and Smart Structures Technologies for Civil, Mechanical, and Aerospace Systems 2007*, vol. 6529. SPIE, 2007, pp. 898–908.
- [14] H. Yousef, M. Boukallel, and K. Althoefer, “Tactile sensing for dexterous in-hand manipulation in robotics—a review,” *Sensors and Actuators A: physical*, vol. 167, no. 2, pp. 171–187, 2011.
- [15] R. L. Truby, C. Della Santina, and D. Rus, “Distributed proprioception of 3d configuration in soft, sensorized robots via deep learning,” *IEEE Robotics and Automation Letters*, vol. 5, no. 2, pp. 3299–3306, 2020.
- [16] O. Kanoun, A. Bouhamed, R. Ramalingame, J. R. Bautista-Quijano, D. Rajendran, and A. Al-Hamry, “Review on conductive polymer/cnts nanocomposites based flexible and stretchable strain and pressure sensors,” *Sensors*, vol. 21, no. 2, p. 341, 2021.
- [17] “Conductive rubber cord stretch sensor + extras!” [Online]. Available: <https://www.adafruit.com/product/519>
- [18] “Adafruit mprls ported pressure sensor breakout - 0 to 25 psi.” [Online]. Available: <https://www.adafruit.com/product/3965>
- [19] “Air pump and vacuum dc motor - 4.5 v and 2.5 lpm.” [Online]. Available: <https://www.adafruit.com/product/4699>
- [20] “Comparison tool for silicone rubbers, urethane rubbers and plastics.” [Online]. Available: <https://www.smooth-on.com/compare/>
- [21] C. Della Santina, R. K. Katzschmann, A. Biechi, and D. Rus, “Dynamic control of soft robots interacting with the environment,” in *2018 IEEE International Conference on Soft Robotics (RoboSoft)*. IEEE, 2018, pp. 46–53.